

# KINEMATIC AND STATIC MODELLING OF THE ADJUSTABLE-BLADE MECHANISM USED IN KAPLAN TURBINES

R. SĂULESCU<sup>1</sup> D. CIOBANU<sup>1</sup> C. JALIU<sup>1</sup>

**Abstract:** *One way to increase the Kaplan turbines performance consists in adjusting the wicket gates angle and the blades angle based on the flow discharge of each specific location. The blades angle can be obtained with different types of mechanisms that allow the blades rotation while the turbine is in operation. Nowadays, the most used mechanisms for blades rotation contain levers connected to a vertical rod, rotating or sliding inside the runner hub. For a good efficiency and to avoid blocking, the blades' driving mechanism has to be analyzed kinematically and statically. Therefore, the paper presents the kinematic and static features of the mechanism of TRRR (T – translation, R - rotation) type used for blades rotation. Numerical simulation of the main kinematic and static parameters is further performed. The optimum dimensions of the levers can be determined in order to minimize the pressure angles values. The simulation results allow establishing geometric and operating requirements for the Kaplan turbine, which are useful for designer and developers in the field.*

**Key words:** *blade angle, driving mechanism, pressure angle, kinematics, statics, hydro, Kaplan turbine.*

## 1. Introduction

The Kaplan turbine is an axial flow reaction turbine that is mainly used in low head applications (2-40 m) on streams with medium to high discharges (0.2 - 40 m<sup>3</sup>/s) [1]. The turbine can operate with fixed or adjustable blades and wicket gates [2]. Thus, the Kaplan turbine is called double-regulated when both the blades and the wicket gates are adjustable. In this case, the runner speed is adapted to any head or discharge variation, operating with a higher efficiency for a wide range of power inputs. Therefore, this is the most flexible Kaplan turbine, working between

15% and 100% of the design discharge. The single-regulated Kaplan turbine allows a good adaptation to variable discharge, as well, working between 30% and 100% of the design discharge [3]. Consequently, one way to increase the efficiency of the Kaplan turbines consists in adjusting the wicket gates angle, and the blade pitch angle, based on the flow discharge of each specific location. The speed and power regulation are obtained with the wicket gates, whose function consists in controlling the discharge going into the runner and adapting the angle of the flow towards the runner blades angle.

---

<sup>1</sup> Centre óRenewable Energy System and Recyclingó, *Transilvania* University of Braşov.

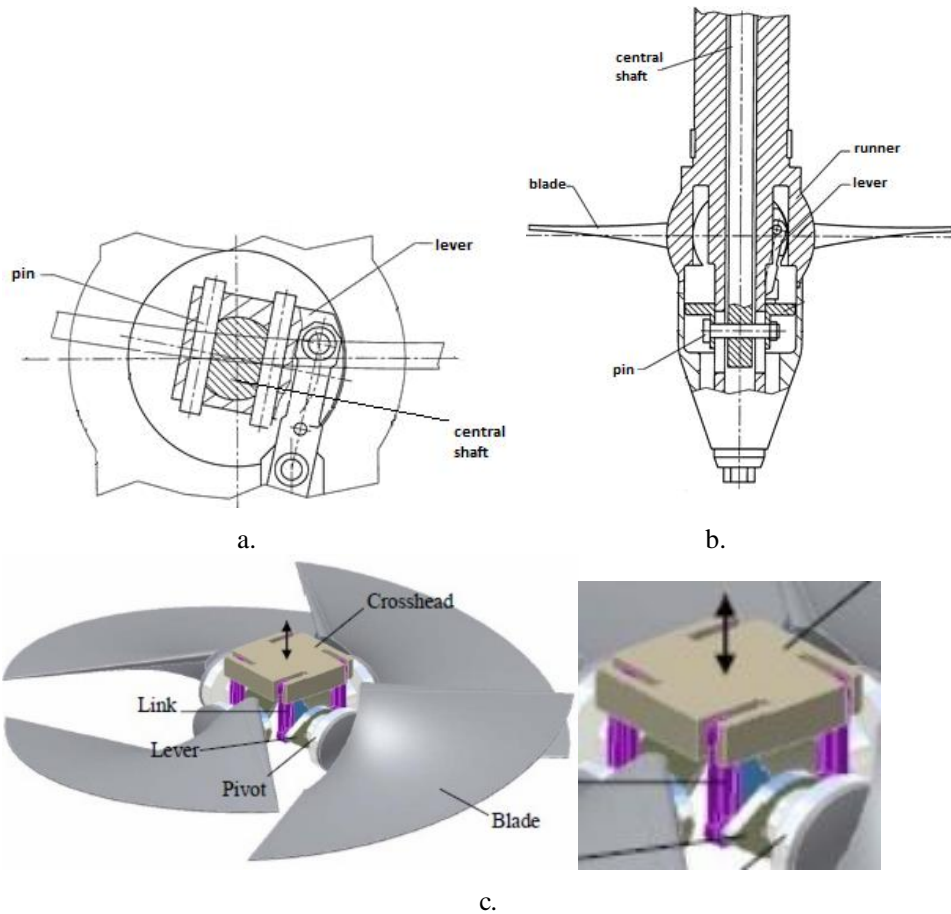


Fig. 1. Mechanisms used for blades rotation: of RRRR type [6] (a), and of TRRR type [7] (b and c)

The wicket gates rotate around their axes due to a rotating mechanism [3]. Besides, the blades angle can be obtained with different types of mechanisms. These mechanisms allow the blades rotation while the turbine is in operation. Generally, the range in which the blades angle takes values is  $16^{\circ}$  (low flows)  $-47^{\circ}$  (high flows) from the horizontal plane [4]. In the early designs, the blades rotation was obtained with a 2D or 3D cam mechanism [4]. Nowadays, other solutions are used, containing levers connected to a vertical rod, rotating (Figure 1,a) or sliding (Figure 1,b and c) inside the runner hub

[5]. Different solutions are presented in the literature [3, 6, 7, 8, 9, 10, 11] with either rotating or sliding input motion. Thus, the driving mechanisms can be of RRRR type or TRRR type.

The wicket gates and blades rotations during turbine operation have to be carefully monitored as their position influence the turbine performance. Therefore, tests had to be performed in order to better control the relative position of the wicket gates and blades and to find the mechanisms singular positions that can lead to blades blocking on the hub. But these tests proved to be expensive and not

to easy to be performed [4]. Therefore, the blocking positions of the adjustable-blade mechanism have to be determined by using a kinematic and static modeling that outlines the values of the pressure angle and the forces on the blades. Consequently, the paper presents the kinematic and static modeling of the most used mechanism for the blades rotation - the mechanism of TRRR type. The optimum dimensions of the levers can be determined in order to minimize the values of the two pressure angles. The results allow establishing operating requirements for the Kaplan turbine, which are useful for designer and developers in the field.

## 2. Kinematic and static modelling of the TRRR mechanism

The most used driving mechanisms for the blades rotation are of crank - rocker (RRRR) and slider ó rocker (TRRR) types. The kinematic and static modelling of the TRRR type mechanism is further presented aiming to optimize the geometry in order to avoid the mechanism blocking. The

structural and kinematic diagrams of the driving mechanism are presented in Figure 2, where the rocker 1 is connected to the blade and the slider 3 is the driving bar. The input parameters are the slider speed  $v_3$  and the driving force  $P_3$ , while the output power is characterized by the rocker speed  $v_1$  and torque  $T_1$ . The dimensions of the bar mechanism are denoted by  $AD = e$ ,  $AB = r$ ,  $BC = l$ , where  $e$  is the mechanism eccentricity (Figure 2a). The blades angle  $\varphi_{10}$  is a function of the slider stroke  $s_{30}$ . As the variation of the blades angle has to be in the range  $16^\circ \text{ ó } 47^\circ$ , the mechanism modelling aims to determine the dependence between the input and output parameters.

Thus, based on the kinematic diagram from Figure 2b, the following relation is obtained:

$$\begin{aligned} e^2 - 2er \sin \varphi_{10} + r^2 \sin^2 \varphi_{10} + s_{30}^2 \\ - 2s_{30}r \cos \varphi_{10} + r^2 \cos^2 \varphi_{10} = l^2 \end{aligned} \quad (1)$$

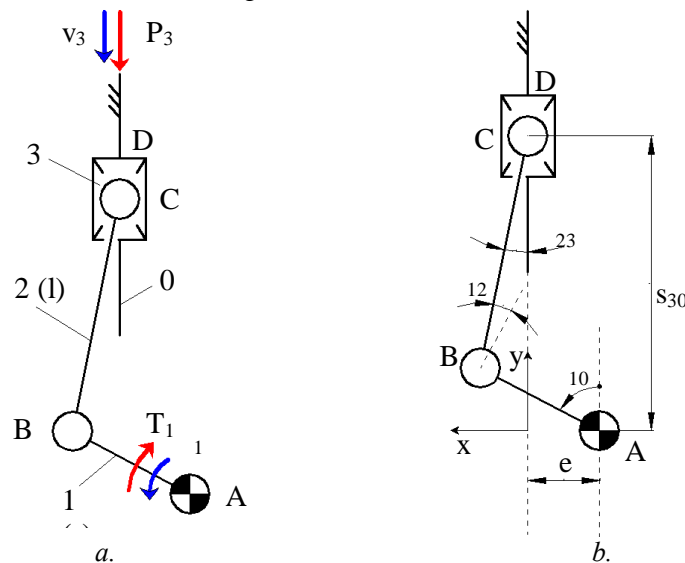


Fig. 2. The structural (a) and kinematic (b) diagrams of the adjustable-blade mechanism

The blades angle can be determined from relation (1) as function of the slider stroke  $s_{30} = s_{30}(\varepsilon)$ :

$$\varphi_{10} = \arcsin(A \cos \varepsilon) - \varepsilon, \quad (2)$$

where the following notations are used:

$$\frac{s_{30}}{e} = \operatorname{tg} \varepsilon, \quad \frac{e^2 + s_{30}^2 + r^2 - l^2}{2er} = A.$$

When imposing the blades angle, the slider position relative to joint A is obtained from relation (2)  $s_{30} = s_{30}(\varphi_{10})$  as follows:

$$s_{30} = r \cos \varphi_{10} + l \sqrt{1 - \left( \frac{e}{l} - \frac{r}{l} \sin \varphi_{10} \right)^2} \quad (3)$$

The pressure angles between the slider 3 and the connecting rod 2, denoted by  $\beta_{23}$  and between the rocker 1 and the connecting rod 2, denoted by  $\beta_{12}$  (Figure 2b) are useful in determining the singular positions in which the mechanism can be blocked. These angles are given by the relations (4) and (5):

$$\beta_{23} = \arcsin \frac{r \sin \varphi_{10} - e}{l} \quad (4)$$

$$\beta_{12} = 90 - (\varphi_{10} + \beta_{23}) \quad (5)$$

The static modelling of the adjustable-blade driving mechanism is based on the following assumption: the friction in the revolute joints is neglected compared to the friction in the sliding joint, due to the use of bearings. Thus, the forces equilibrium equations for the rocker and the slider can be written based on the diagram from Figure 3 (F is the reaction force in the revolute joint, acting along the connecting rod):

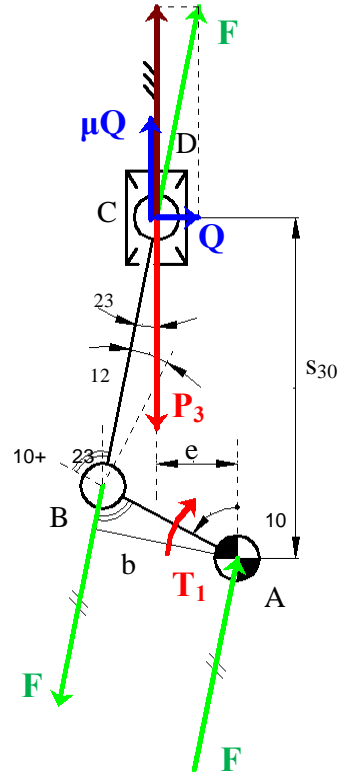


Fig. 3. The diagram used in the static modelling

- the rocker:

$$T_1 - Fb = 0; \quad F = \frac{T_1}{b}; \quad (6)$$

$$b = r \sin(\varphi_1 + \beta_{23});$$

- the slider:

$$Q - F \sin \beta_{23} = 0;$$

$$Q = \frac{T_1 \sin \beta_{23}}{r \sin(\varphi_1 + \beta_{23})};$$

$$P_3 - F \cos \beta_{23} - \mu Q = 0;$$

$$P_3 = \frac{T_1 \cos \beta_{23}}{r \sin(\varphi_1 + \beta_{23})} + \mu Q. \quad (7)$$



be obtained from Figure 5, b and c.

Based on relation (6) and (7), the driving force  $P_3$  can be determined as function of the torque on the blade shaft  $T_1$  (the torque generated by the water power), for a friction coefficient in the sliding joint  $\mu=0.1$  (steel). The required force and the friction force in the sliding joint (the linear actuator) can be obtained as function of the torque  $T_1$  and the blades rotation stroke.

The diagrams from Figure 6a present the dependence of the reduced force  $P_3^*=P_3/r$  on the slider reduced position  $s_{30}^*$  for different values of the torque that rotates the blades  $T_1$ . The reduced reaction force  $Q^*=Q/r$  and the friction force in the sliding joint  $Q$ , respectively, can be determined as functions of the slider reduced position  $s_{30}^*$  from the numerical simulations presented in Figure 6b.

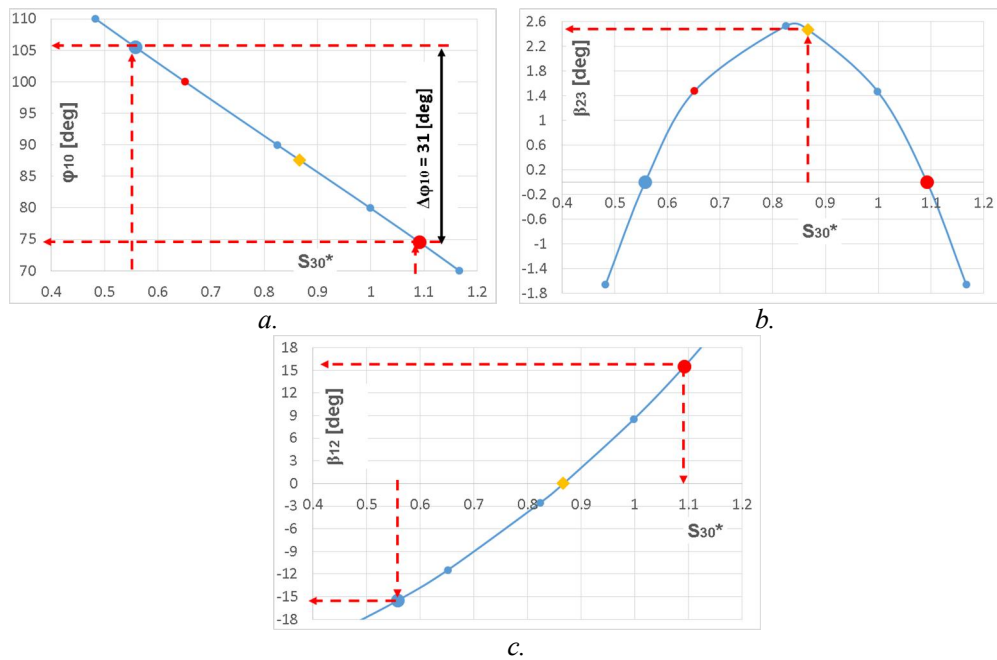
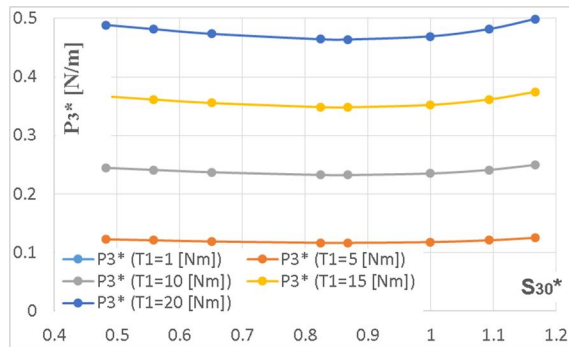
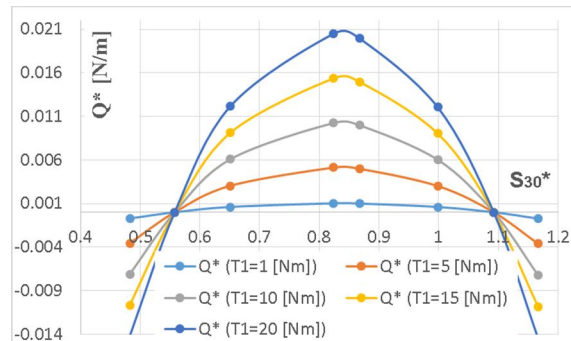


Fig. 5. Numerical simulations for: the blades angles  $\varphi_{10}$  (a), the pressure angle  $\beta_{23}$  (b) and the pressure angle  $\beta_{12}$  (c) versus the slider reduced position  $s_{30}^*$



a.



b.

Fig. 6. Numerical simulations for: the reduced driving force (a), and the reduced reaction force (b) as function of the reduced slider position for different values of the torque that rotates the blades

#### 4. Discussions and conclusions

The results of the numerical simulations allow highlighting the following conclusions:

- the dimensions of the adjustable-blade mechanism can be determined from the diagram in Figure 5,a by imposing the blades stroke and minimum values of the pressure angles, and by adopting the rocker and connecting rod lengths in relation to the turbine dimensions; the other geometrical parameters can be obtained by using rel. (1) and (3);
- the values of the pressure angles between the rocker and the connecting rod  $\varphi_{12}$  and between the slider and the connecting rod  $\varphi_{23}$  should be as small as possible, being important for the correct functioning of the driving mechanism;
- for a correct functioning and a higher reliability of the adjustable-blade mechanism, the eccentricity should be determined as function of the rocker and connecting rod lengths for minimum values of the pressure angles  $\varphi_{12}$  and  $\varphi_{23}$ . For instance, the rocker rotation angle  $\varphi_{10}$  can

be obtained for an imposed rocker stroke  $\Delta\varphi_1$  and minimum values of the two pressure angles, in module; to minimize the values of these angles, the blades' angular stroke should be symmetrical to the horizontal plane;

- the driving force  $P_3$  increases with the increase of the torque required to rotate the blades,  $T_1$  (for the numerical case, the force variation is a parabolic function, with an increment of 5 at the stroke ends). The force takes smaller values for the blades' angle in the range  $50^\circ \text{ to } 180^\circ$  relative to the horizontal plane. Thus, the motor that is required to actuate all the blades will be characterized by a smaller power;
- the friction force in the sliding joint is maximum for the horizontal position of the blades (Figure 6b) and increases with the increase of the torque  $T_1$ ; the use of a motor with lower power leads to an increased efficiency of the driving mechanism;
- in the hypothesis of using bearings in the revolute joints, the friction force in the sliding joint is maximum when the rocker is orthogonal on the sliding direction and increases with the increase of the torque  $T_1$ ;

- in most of the structural cases, the relation between the two pressure angles is  $|\alpha_2| > \alpha_{23 \max}$ . For a mechanism with known lever dimensions, its eccentricity is chosen so that  $|\alpha_2| \dot{\theta}_{12 \max \text{ adm}}$ , and  $|\alpha_2 \max| = |\alpha_2 \min|$ , respectively, at the slider stroke ends.

The simulation results are useful to the designers and developers in the field for dimensioning the blades of driving mechanism under the requirement of correct functioning.

### References

1. Penche, C., *Layman's Handbook on How to Develop a Small Hydro Site*, Second Edition, European Small Hydro-Power Association (ESHA), 1998.
2. Pelikan, B. et al., *Guide on How to Develop a Small Hydropower Plant*, ESHA, 2004.
3. Visa, I., Jaliu, C., Duta, A., Neagoe, M., Comsit, M., Moldovan, M., Ciobanu, D., Burduhos, B., Saulescu, R., *The Role of Mechanisms in the Sustainable Energy Systems*, Transilvania University Publishing House, 2015.
4. Albright, D. *Automatic Index Test Box for Kaplan Turbines*, 2012, <http://www.actuationtestequipment.com> /Accessed:08.06.2016).
5. Buchelt, B. *Blade for Kaplan turbine*, Patent US 6007297 A, 1998.
6. Patent RU 2209338. *The impeller Kaplan turbine*.
7. Patent RU 2193105. *Rotor of the turbine*.
8. Patent US 6533536 B1. *Hydro-turbine runner*.
9. Patent US 3226084 A. *Adjustable blade propeller type pumps and pump turbines*.
10. Patent RU 2395710. *Blade adjustment mechanism of impeller of adjustable-blade propeller turbine*.
11. Patent US 3822104. *Plug and seal design for adjustable blade propeller turbine*.